95CH35810

Jim Sturm
Princeton Univ
609-258-5610
sturm@ee.princeton.edu

international ELECTRON DEVICES meeting

1995

WASHINGTON, DC
DECEMBER 10–13, 1995

TECHNICAL DIGEST

Sponsored by Electron Devices Society of IEEE

Numerical Simulation of the Temperature Dependence of Band-Edge Photoluminescence and Electroluminescence in Strained-$Si_{1-x}Ge_x$/Si Heterostructures

A. St.Amour and J.C. Sturm
Department of Electrical Engineering
Princeton University
Princeton, NJ 08544

ABSTRACT

The temperature dependence of band-edge photoluminescence (PL) and electroluminescence (EL) of $Si_{1-x}Ge_x$/Si heterostructures was simulated using a two-carrier device simulator. The device simulator was used to determine electrically and optically excited carrier profiles, from which light emission was computed. The simulations confirmed an earlier result that PL intensity at high temperature (>150K) is controlled by surface recombination. Furthermore, it was found that the difference in measured temperature dependence between PL and EL experiments is due to (i) the EL experiments being performed at a much higher total injection rate and (ii) the heavily doped, buried contact layers in EL structures (p-i-n diodes) effectively blocking carriers from diffusing into the substrate and away from the $Si_{1-x}Ge_x$ layer.

INTRODUCTION

Strained-$Si_{1-x}Ge_x$/Si heterostructures are attractive as potential IR emitters because of their compatibility with existing Si processing technology. To date, several groups have measured electroluminescence (EL) from $Si_{1-x}Ge_x$ quantum well or Ge/Si superlattice light emitting diodes (1-5). The available data has consistently shown that the EL intensity from such structures persists to higher temperature than does the band-edge photoluminescence (PL) from similar structures, but no explanation has yet been given for this phenomenon.

Here, we report what we believe are the first two-carrier, numerical simulations of $Si_{1-x}Ge_x$/Si heterostructures designed to understand the temperature dependence of the luminescence intensity under either optical or electrical pumping. Numerical simulation is required to modelled this behavior because of the complicated nature of the problem. For example, accurate modelling of free carrier distributions (which determine luminescence intensity) during optical pumping must take into account exponentially decaying photogeneration, temperature dependent electron and hole diffusion, unequal lifetimes in different materials (and at interfaces), band bending due to charge accumulation, and effects of high carrier concentration (such as Auger recombination and degeneracy).

The one-dimensional simulations were performed with a commercial two-carrier, heterojunction device simulator, which can accomodate optical carrier generation (TMA Medici). Two structures were simulated from 100 to 350K. The first was a single buried 5nm $Si_{0.65}Ge_{0.35}$ quantum well with a 20nm Si cap (Fig. 1a); the second was a p-i-n diode with a single 5nm $Si_{0.65}Ge_{0.35}$ quantum well within the i region (Fig. 1b). For the PL simulations, the absorption length of the pump was 1μm. The model chosen in the simulator included both Shockley-Read-Hall and Auger recombination. For simplicity, the electron and hole SRH lifetimes (τ_{SRH}) were assumed to be 1μs throughout both structures, and the Auger recombination coefficients (C_n and C_p) were 2.8×10^{-31} and $9.9\times10^{-32}cm^6s^{-1}$, for electrons and holes, respectively. Throughout the samples then, recombination was modelled by

$$U = \frac{pn - n_i^2}{\tau_{SRH}\cdot(n + p + 2n_i)} + C_n(pn^2 - nn_i^2) + C_p(np^2 - pn_i^2). \quad (1)$$

Having simulated the electron and hole distributions, we then used them to calculate the luminescence intensity. In general, one can write that the luminescence intensity from the $Si_{1-x}Ge_x$ is given by

$$I_{SiGe} = \int B\cdot np\cdot dx \quad (2)$$

where B is the Einstein spontaneous emission coefficient and is generally a function of n, p, and temperature (6). The integral is evaluated over the width of the $Si_{1-x}Ge_x$ layer. However, at carrier densities above the Mott transition (7), the luminescence is no longer from discrete excitons but rather from an electron-hole plasma (8). At these high carrier densities, the radiation is proportional to the pn product because, through either the phonon-assisted recombination or the no-phonon recombination process in $Si_{1-x}Ge_x$ alloys, any conduction band electron can recombine with equal probability with any valence band hole. Furthermore, B should not be a strong function of temperature in this regime because excitons do not play a significant role.

0-7803-2700-4 $4.00

Temperature Dependence of PL Intensity

Qualitatively similar temperature dependence of PL from as-grown $Si_{1-x}Ge_x$ quantum wells with Si caps has been observed in several experiments (3, 9-11). These authors all reported relatively constant PL intensity at low temperature and sharply decreasing intensity at higher temperatures. In an earlier paper, we experimentally showed that the high temperature luminescence intensity could be enhanced by more than an order of magnitude by passivating the top Si surface with oxide (12). We showed that the degradation of the luminescence with increasing temperature was due, not to a property of the $Si_{1-x}Ge_x$ itself, but to recombination at the top Si surface as carriers were thermally excited from the well.

In Fig. 2, we have simultaneously plotted measured luminescence intensity and simulated pn product as a function of inverse temperature for two sets of PL data. Each data set was independently scaled to overlay its corresponding simulation at low temperature. At low temperature ($T < 150K$), nearly all of the photogenerated carriers were trapped in the $Si_{1-x}Ge_x$ well so that the $Si_{1-x}Ge_x$ PL intensity was constant and its absolute intensity was controlled by the carrier lifetime in the $Si_{1-x}Ge_x$. As the temperature was increased and carriers were thermally excited from the well, the fraction of carriers in the $Si_{1-x}Ge_x$ decreased, but the $Si_{1-x}Ge_x$ PL began to decay well before a majority of the carriers were in Si because the total number of carriers in the system decreased due to the very low effective lifetime in the Si, which includes top-surface recombination.

To reduce the recombination at the top surface, the samples were thermally oxidized. Of the two data sets in Fig. 2, the "knee" is clearly at a higher temperature for the sample with oxide passivation. By only changing the top surface recombination velocities (S_n and S_p), the simulation was able to accurately reproduce this behavior. For the sample with oxide passivation, a simulated recombination velocity less than 10^3cm/s was required to fit the data; while for the sample without oxide, the simulated recombination velocity was 10^5cm/s.

Fig. 3 shows the band diagram and carrier distribution in the near-surface region from a PL simulation at 200K. Note that the quasi-fermi levels were flat indicating that the carrier profiles were determined by quasi-equilibrium, not kinetics. That is, the electron and hole populations in the $Si_{1-x}Ge_x$ were in equilibrium with their corresponding populations in the Si cap and in the top of the substrate. Also, note that there is considerable band bending due to the accumulated holes in the quantum well.

Comparison of PL and EL

Electroluminescence data (1) and its simulation appears in Fig. 2 along with the PL data and simulation. Note the relatively flat temperature dependence compared to PL, which was the chief motivation for this study. We found two reasons for the difference. First, the electron and hole densities in the EL simulations were noticably higher than those in the PL simulations. This was due to the much higher injection rate for the EL measurements, which were performed at a drive current density of $280A/cm^2$. This corresponds to a pump rate 4000 times higher than that during the PL measurements. That the pn product at low temperature was only about 200 times higher for the EL simulation than for PL simulation is due to Auger recombination, which dominated the carreir lifetime at high densities.

Auger recombination had its greatest effect at low temperature as the electron and hole concentrations in the $Si_{1-x}Ge_x$ were at their highest levels. Auger recombination became less important as the temperature increased and the densities decreased. This had the effect of flattening the temperature dependence of the pn product in the $Si_{1-x}Ge_x$ and consequently flattening the temperature dependence of the EL.

To make an honest comparison between PL and EL, we simulated the two cases at the same injection level verses temperature. That meant reducing the EL drive current to $0.067A/cm^2$. (The PL photogeneration rate was $4.2x10^{17}cm^{-2}s^{-1}$.) From these simulations, the pn product in the $Si_{1-x}Ge_x$ is plotted in Fig. 4 as a function of inverse temperature. Owing to the equal injection rates, the pn product had the same value ($5x10^{29}cm^{-5}$) for $T < 150K$. However, at higher temperatures, there were many more carriers in the $Si_{1-x}Ge_x$ for the EL case than for the PL case. Consequently, the EL would be stronger than the PL, and thus the EL "knee" is pushed out to higher temperature.

Recall that the quasi-fermi levels in the PL simulations were flat in the near-surface region (see Fig. 3). In fact, the quasi-fermi levels were nearly flat to more than 50μm into the substrate for the PL simulations. As stated earlier, this indicates that the carrier populations in the $Si_{1-x}Ge_x$ were very near quasi-equilibrium with those in the Si. In such a case, the integrated pn product in $Si_{1-x}Ge_x$ (from which we derive luminescence intensity) can be expressed by

$$(pn)_{SiGe} = \frac{W_{SiGe}}{W_{Si}} \cdot (pn)_{Si} \cdot \exp(-\Delta E_G / kT) \qquad (3)$$

where W_{SiGe} is the width of the $Si_{1-x}Ge_x$ layer, W_{Si} is the effective width of the Si, and ΔE_G is the bandgap difference between Si and $Si_{1-x}Ge_x$. W_{Si}(PL) is on the order 50μm, while W_{Si}(EL) is equal to the width of the intrinsic layer of the p-i-n diode (0.56μm). As a result, referring to (3) we then expect a much higher $(pn)_{SiGe}$ and luminescence intensity in the EL case compared to the PL case. The difference in effective Si widths is

demonstrated in Fig. 5, which shows the pn product as a function of depth. For the PL simulation, pn was significant deep into the substrate, whereas, for the EL simulations, pn was quite small except within the top few microns.

The importance with respect to temperature dependence of the i-Si layer thickness was confirmed by performing simulations for which it was varied. Included on Fig. 4 is the simulated pn product for a thicker bottom i-Si spacer (1.4μm vs. 0.4μm). The effect of the thicker i-Si layer was to shift the EL "knee" towards lower temperature and towards the PL "knee".

SUMMARY

We have shown that a two-carrier electronic device simulator can be used to understand the temperature dependence of photo- and electroluminscence in $Si_{1-x}Ge_x$ heterostructures. We have indentified two causes for the experimentally observed difference in temperature dependence between PL and EL. First, the pump rates in EL experiments are typically much higher than those in PL experiments, resulting in higher carrier concentrations and thus more Auger recombination (especially at low temperature) in the EL case. Second, the effective Si width over which the $Si_{1-x}Ge_x$ shares the injected carriers is orders of magnitude larger in PL experiments than in EL experiments. This second cause suggests that for best room temperature EL efficiency the thickness of the undoped Si spacers in a $Si_{1-x}Ge_x$ quantum well p-i-n diode should be minimized.

REFERENCES

(1) Q. Mi, X. Xiao, J.C. Sturm, L.C. Lenchyshyn, and M.L.W. Thewalt, "Room-temperature CW 1.3μm and 1.5μm electroluminescence from Si/SiGe quantum wells," *IEEE Dev. Res. Conf. Proc.*, VIB.7, 1992.

(2) D.J. Robbins, P. Calcott, and W.Y. Leong, "Electroluminescence from a pseudomorphic SiGe alloy," *Appl. Phys. Lett.* 59, p. 1350, 1991.

(3) M. Gail, J. Brunner, U. Menczigar, A. Zrenner, and G. Abstreiter, "Luminescence studies of MBE grown Si/SiGe quantum wells," *Mat. Res. Soc. Symp. Proc.* 298, p. 21, 1993.

(4) J. Engvall, J. Olajos, H.G. Grimmeiss, H. Presting, H. Kibbel, and E. Kasper, "Electroluminescence at room temperature of a Si/Ge strained-layer superlattice," *Appl. Phys. Lett.* 63, p. 491, 1993.

(5) J. Olajos et al, "Photo- and electroluminescence in short-period Si/Ge superlattice structures," *Semi. Sci. Tech.* 9, p. 2011, 1994.

(6) H. Schlangenotto, H. Maeder, and W. Gerlach, "Temperature Dependence of the Radiative Recombination Coefficient in Silicon," *Phys. Stat. Sol.* A21, p. 357, 1974.

(7) E. Cohen, M.D. Sturge, M.A. Olmstead, and R.A. Logan, "Electron-hole plasmas in photoexcited indirect-gap AlGaAs," *Phys. Rev.* B22, p.771, 1980.

(8) X. Xiao, C.W. Liu, J.C. Sturm, L.C. Lenchyshyn, and M.L.W. Thewalt, "Photoluminescence from electron-hole plasmas confined in Si/SiGe/Si quantum wells," *Appl. Phys. Lett.* 60, p. 1720, 1992.

(9) S. Fukatsu, N. Usami, and Y. Shiraki, "Luminescence from strained SiGe/Si quantum wells grown by Si molecular beam epitaxy," *Jpn. J. Appl. Phys.* 32, p. 1502, 1993.

(10) M. Wachter, F. Schaffler, H.-J. Herzog, K. Thonke, and R. Sauer, "Photoluminescence of high-quality SiGe quantum wells grown by molecular beam epitaxy," *Appl. Phys. Lett.* 63, p. 376, 1993.

(11) J.C. Sturm, A. St.Amour, Q. Mi, L.C. Lenchyshyn, and M.L.W. Thewalt, "High temperature (77-300K) photo- and electroluminescence in Si/SiGe heterostructures," *Jpn. J. Appl. Phys.* 33, p. 2329, 1993.

(12) A. St.Amour, J.C. Sturm, Y. Lacroix, and M.L.W. Thewalt, "Enhancement of high-temperature photoluminescence in strained-SiGe/Si heterostructures by surface passivation," *Appl. Phys. Lett.* 65, p. 3344, 1994.

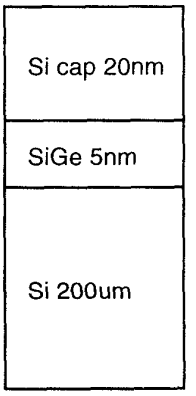

Fig. 1a. PL structure.

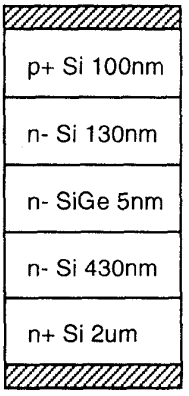

Fig. 1b. EL structure.

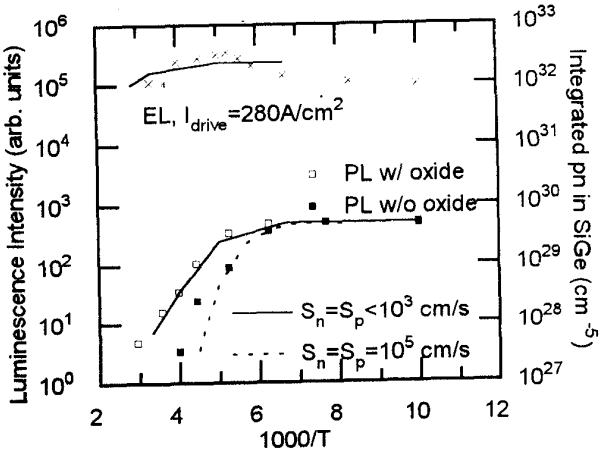

Fig. 2. Integrated luminescence intensity (x, □, ■) and simulated pn product (lines) as a function of inverse temperature.

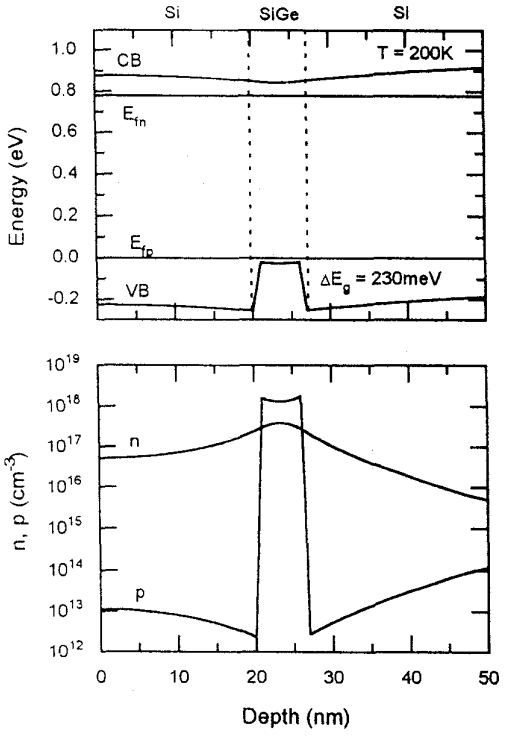

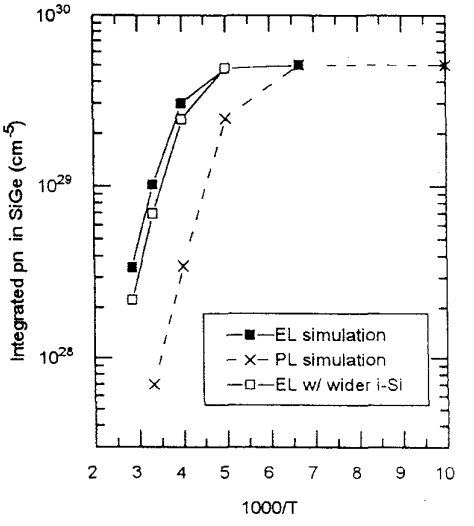

Fig. 4. Simulated pn product as a function of inverse temperature.

← Fig. 3. Band diagram and carrier distribution for PL simulation at 200K. $S_n = S_p = 0$.

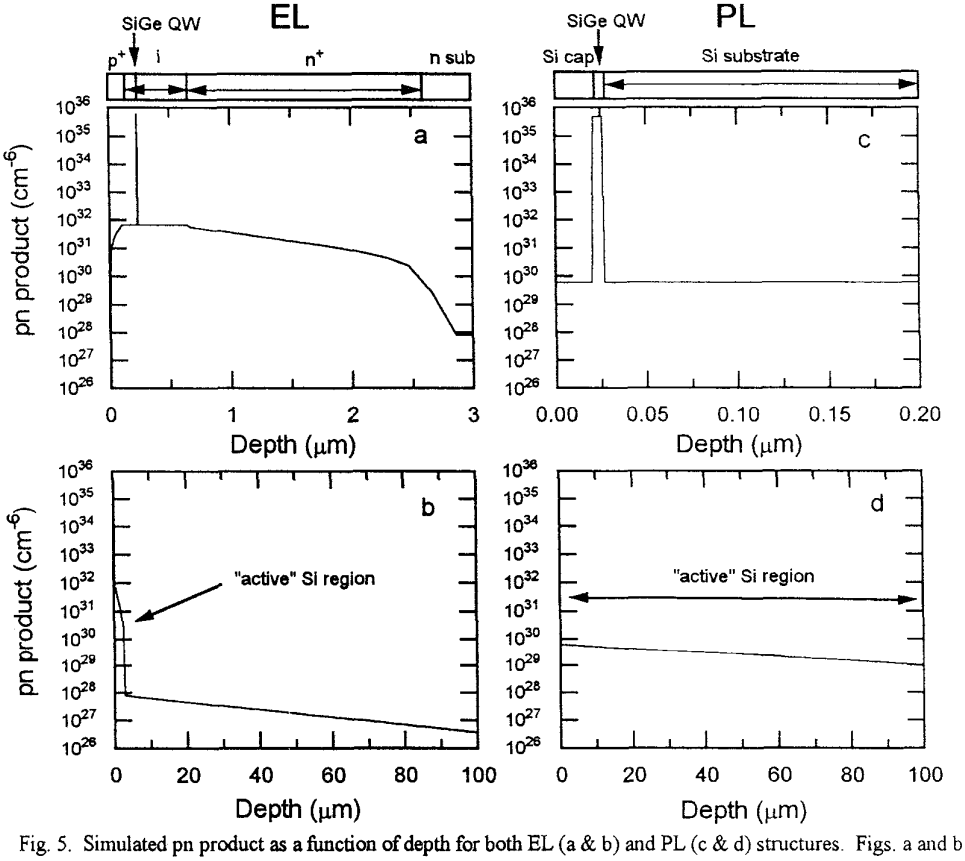

Fig. 5. Simulated pn product as a function of depth for both EL (a & b) and PL (c & d) structures. Figs. a and b show the same EL simulation at different depth scales. Figs. c and d show the same PL simulation. The carrier injection rate was identical in both cases. Note that the QW pn spikes are not visible on the 100um depth scale.